Journal of Thermal Analysis, Vol. 53 (1998) 697-709

PHASE DIAGRAM OF *R*(+)-*S*(−) EFAROXAN HYDROCHLORIDE

R. Pena[1*], *A. Chauvet*[1], *J. Masse*[1], *J. P. Ribet*[2] *and J. L. Maurel*[2]

[1]Faculté de Pharmacie Laboratoire de Chimie Générale et Minérale, 15, avenue Charles Flahault 34060, Montpellier cedex 2
[2]Centre de Recherche Pierre Fabre, Département de Chimie Analytique, 17, avenue Jean Moulin 81106 Castres cedex, France

(Received October 13, 1997)

Abstract

The phase diagram of *R*(+)-*S*(−) efaroxan hydrochloride ($T_{fus.}(R)$=245.1±0.3°C. $\Delta H_{fus.}(R)$= 119.6±3.0 J g^{-1}) shows a racemic compound. The melting temperature and melting enthalpy of the compound are: $T_{fus.}(RS)$=247.8±0.2°C and $\Delta H_{fus.}$ (*RS*)=124.6±2.4 J g^{-1}. A solid ↔ solid transformation takes place at $T_{trs.}$=180±1°C, $\Delta H_{trs.}$=15.0±0.4 J g^{-1}. This transition is observed between 3 and 97% *R*(+). The stability of the racemic compound already established in a previous study was confirmed by the value of Petterson's coefficient (*i*=1.19). The two eutectic positions at 20 and 80% *R*(+) that define the range over which the racemic compound is found, exclude the use of resolution methods by preferential crystallization.

Keywords: DSC, efaroxan hydrochloride, phase diagram, racemic compound

Introduction

The biological activity of a drug often depends on its stereochemistry. Studies of chiral molecules have shown that two enantiomers of the same molecule may have different pharmacologic and pharmacokinetic properties [1–5].

R(+) efaroxan hydrochloride [6] is a potent and highly selective α2 adrenoreceptor antagonist. It increases the endogenous acetylcholine flow in the medial prefontal cortex in the rat [7]. A previous study has shown that an equimolar mixture of *R*(+) and *S*(−) enantiomers crystallizes into a racemic compound that gives a solid ↔ solid transition at 180±1°C(ΔH_{trs}=15.0±0.4 J g^{-1}) [8].

The phase diagram between *R*(+) and *S*(−) enantiomers is characteristic of a racemic compound [9] and can be used to decide whether optical resolution by preferential crystallization is feasible [9, 10]. Generally, this technique is less expensive than the asymmetric organic synthesis or the formation of diastereoisomers.

* Author for correspondence: phone: 0467548081; fax: 0467548039.

1418–2874/98/ $ 5.00

Akadémiai Kiadó, Budapest
Kluwer Academic Publishers, Dordrecht

We calculated the phase diagram using the Prigogine-Defay and Schröeder-Van Laar equations [11]. The advantage of this approach is that it confirms the experimental results and, in some cases can predict phase equilibria when experimental methods are insufficient for their description.

Experimental

Apparatus

Differential scanning calorimetry

DSC profiles were obtained on a Mettler FP 800 thermal analyser fitted with an Epson HX 20 microcomputer, a FP 85 measuring cell and a FP 80 HT temperature controller.

Thermomicroscopy

A Leitz SM POL microscope connected to a FP52 hot stage and a Mettler FP5 temperature controller were used for microscopic investigations. Observations were videotaped using a Sony DXC-101P color video camera connected directly to the microscope.

Operating conditions

In studies by differential scanning calorimetry the samples (3–5 mg) were introduced into a 40 µl aluminium crucible. Sealed and perforated crucibles were heated at 5°C min^{-1} under a stream of nitrogen (20 ml min^{-1}). The melting temperature was determined according to I.U.P.A.C. norms and corresponded to the extrapolated onset temperature. Melting enthalpies and temperatures were determined in five experiments using sealed but non perforated crucibles. The mean and standard error were calculated from five experimental values.

The apparatus was calibrated using the melting enthalpy of indium (28.5 J g^{-1}) used as a reference [12]. The melting temperature of the eutectic point was evaluated from the mean values and standard errors calculated from the overall results obtained for each composition.

In studies by thermomicroscopy, the heating and cooling rates were 10°C min^{-1} and 2 or 3°C min^{-1} near the melting point.

Microthermoanalysis and contact methods have also been used [13]. After the diffusion of melted substances and their crystallization, the phases formed in the interaction area are displayed and their melting temperatures determined.

Reagents

Efaroxan hydrochloride ($C_{13}H_{17}N_2O^+Cl^-$, M=252.5 g mol^{-1}) was synthesized by the Pierre Fabre Laboratory. The enantiomers were soluble in water (1200 mg ml^{-1}) and methanol (600 mg ml^{-1}). The *R*(+) and *S*(–) enantiomers

were resolved by preferential crystallization of diastereoisomer salts obtained with dibenzoyl tartaric acid.

Enantiomeric purity was evaluated by HPLC and was better than 99.2%.

As polymorphism has an effect on the phase diagram, we started by studying the thermal behaviour of each reagent by thermal and spectral analyses [8].

Physical mixtures were obtained by grinding precisely weighted small quantities of *R*(+) enantiomer and *RS* racemic compound. The coprecipitates were prepared by dissolving the physical mixtures in 6–7 ml of boiling acetonitrile. They were then recrystallized by evaporation of the solvent at room temperature.

We checked that the energetic contribution provided by grinding and crystallization did not modify polymorphism. As the thermodynamic properties of the antipodes were identical [14], we restricted our experiments to a study of mixtures made up of *R*(+) enantiomer and the racemic compound (*RS*).

The mole fractions were thus:

– x_R mole fraction of (*R*) in the binary *R/S*,
– x_S mole fraction of (*S*) in the binary *R/S*,
– X_{RS} mole fraction of (*RS*) in the binary *RS/R*,
– X_R mole fraction of (*R*) in the binary *RS/R*.

$$X_R = 2x_R - 1 \quad \text{when} \quad 0.5 > x_R > 1 \tag{1}$$

It should be noted that the mole and mass fractions are identical because the two enantiomers have the same molecular weight.

Experimental results

Melting temperatures and enthalpies for the enantiomers and racemic compound are listed in Table 1 [8]. Crystallographic data for the enantiomers [6] and racemic compound [15] are given in Table 2. Figure 1 shows the DSC curves of the pure constituents and six binary compositions (*RS/R*) containing 20, 30, 40, 60, 80, 90% *R* obtained using the coprecipitate method.

Table 1 Melting points and enthalpies of fusion for the enantiomers and the racemic compound

	Melting temperature/ °C	Melting enthalpy/ J g^{-1}
Enantiomers	245.1±0.3	119.6±3.0
Racemic compound	247.8±0.2	124.6±2.4

The DSC curves show two endothermic processes, eutectic fusion and liquidus. These results are presented in Tables 3 and 4. The phase diagrams are shown in Fig. 2a, b.

Table 2 Crystallographic data of the enantiomers and the racemic compound

	Enantiomers	Racemic compound
Space group	$P2_1$	P_1^-
System	monoclinic	triclinic

The II ↔ I transition of the racemic compound indicated by DSC is represented in Fig. 3. This transition occurs at $T_{trs.}$=180±1°C with an enthalpy $\Delta H_{trs.}$= 15.0± 0.4 J g^{-1}. Tammann's diagrams of solid ↔ solid transition are very close (Fig. 4), y=–0.94613+13.946x (r^2=0.993) for the physical mixtures and y= –1.0471+14.045x (r^2=0.995) for the coprecipitates. This result indicates no solid solution between 3.4 and 50%*R* for the physical mixtures and between 3.8 and 50%*R* for the coprecipitates.

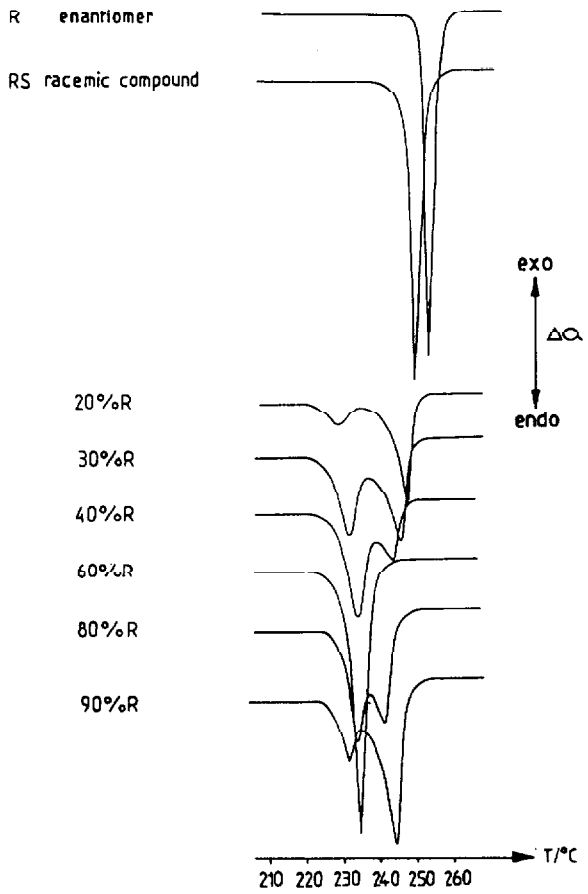

Fig. 1 DSC curves of (*R*) enantiomer, *RS* racemic compound and six binaries obtained by the coprecipitate methods

Tammann's diagrams of the eutectics are plotted for each binary *RS/R* mixture in Fig. 5. No solid solution was observed between 54.0–96.5%*R* for the physical mixtures and between 56.7–97.5 %*R* for the coprecipitates.

The intersection point of the two straight lines ($\Delta H_{fus.}(eut.)=f(x_R^1)$) gave the eutectic composition of the binary *RS/R*.

Physical mixtures: $\Delta H_{fus.}(eut.)= -12.5+140.9X_R$ with $r^2=0.954$
$\Delta H_{fus.}(cut.)= 175.9-190.0X_R$ with $r^2=0.997$
Coprecipitates: $\Delta H_{fus.}(eut.)=-23.6+177.0X_R$ with $r^2=0.994$
$\Delta H_{fus.}(eut.)=231.9-243.2X_R$ with $r^2=0.945$

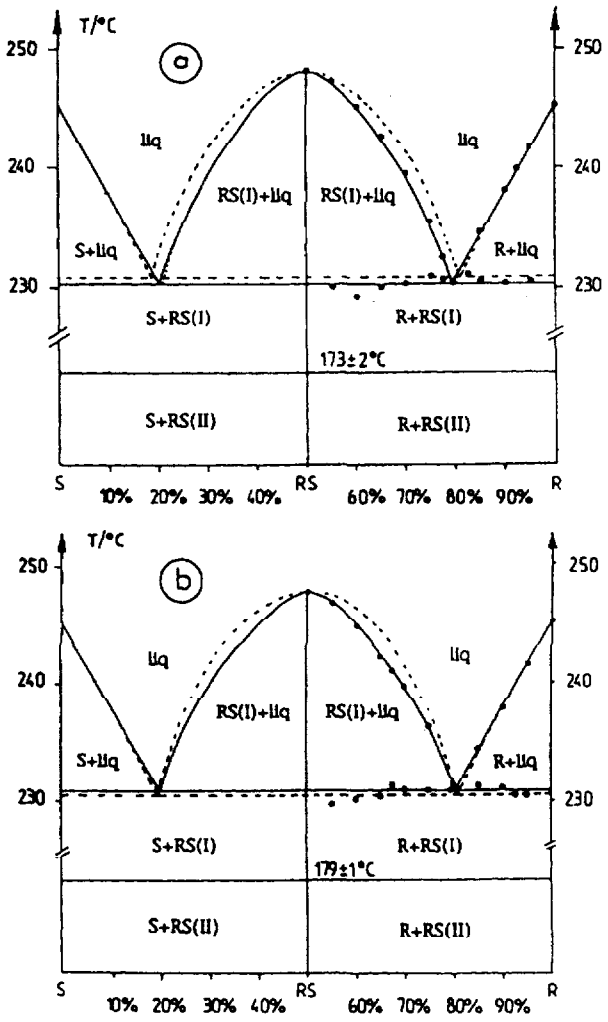

Fig. 2 Phase diagrams: a – physical mixtures; b – coprecipitates

Table 3 DSC data of physical mixtures

Composition				Eutectic		Liquidus
X_{RS}	X_R	x_R	x_S	T/°C	ΔH/J g^{-1}	T/°C
1.000	0.000	0.500	0.500			247.8±0.2
0.900	0.100	0.550	0.450		2.7	246.8±0.5
0.800	0.200	0.600	0.400	229.2	11.5	245.0±0.5
0.700	0.300	0.650	0.350	230.0	34.8	242.5±0.4
0.600	0.400	0.700	0.300	230.3	41.9	239.4±0.1
0.500	0.500	0.750	0.250	230.9		235.4±0.3
0.450	0.550	0.775	0.225	230.6		232.5±0.3
0.410	0.590	0.795	0.205	230.3		
0.400	0.600	0.800	0.200	231.1		
0.300	0.700	0.850	0.150	230.5		235.4±0.4
0.200	0.800	0.900	0.100	230.3	23.6	238.0±0.1
0.150	0.850	0.925	0.075	230.3	15.0	239.8±0.6
0.100	0.900	0.950	0.050	230.2	4.6	241.6±0.8
0.000	1.000	1.000	0.000			245.1±0.3

Table 4 DSC data of coprecipitates

Composition				Eutectic		Liquidus
X_{RS}	X_E	x_R	x_S	T/°C	ΔH/J g^{-1}	T/°C
1.000	0.000	0.500	0.500	–	–	247.8±0.2
0.900	0.100	0.550	0.450	–	–	246.8±0.4
0.800	0.200	0.600	0.400	230.0	12.3	244.8±0.3
0.700	0.300	0.650	0.350	230.3	29.3	242.2±0.4
0.650	0.350	0.675	0.325	231.2	37.0	241.0±0.4
0.600	0.400	0.700	0.300	230.9	48.4	239.6±0.5
0.500	0.500	0.750	0.250	230.8	–	236.2±0.5
0.450	0.550	0.775	0.225	231.3	–	234.0±0.7
0.410	0.590	0.795	0.205	230.8	–	–
0.380	0.620	0.810	0.190	231.0	–	–
0.300	0.700	0.850	0.150	231.2	58.5	234.2±0.4
0.200	0.800	0.900	0.100	231.0	44.8	237.8±0.6
0.100	0.900	0.950	0.050	230.4	11.0	241.5±0.1
0.000	1.000	1.000	0.000	–	–	245.1±0.3

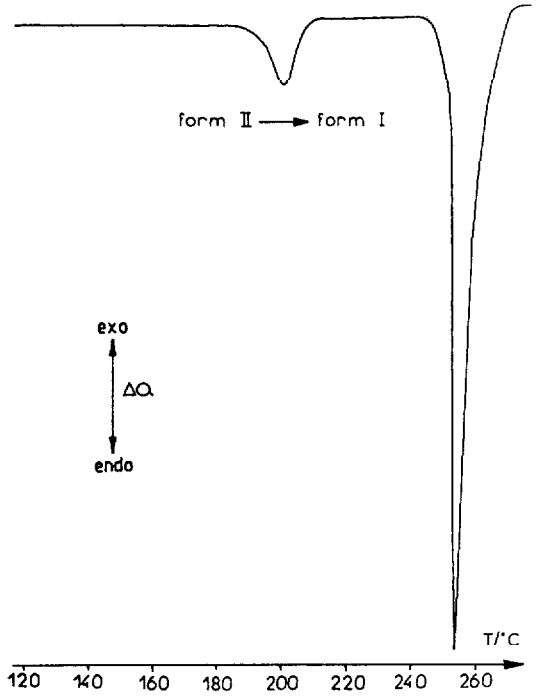

Fig. 3 DSC curves of the racemic compound showing the solid ↔ solid transition and the fusion

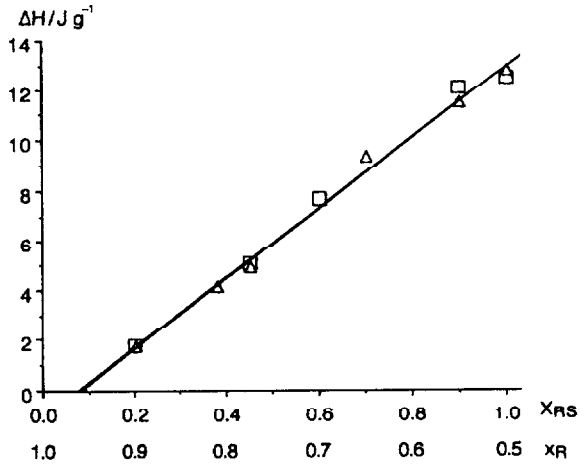

Fig. 4 Tammann diagram of solid ↔ solid transition: □ – physical mixtures, Δ – coprecipitates

In the phase diagram of *R/RS* cutectic compositions of X_{R_e}=0.57 and 0.61 were determined for the physical mixtures and the coprecipitates. As the thermo-

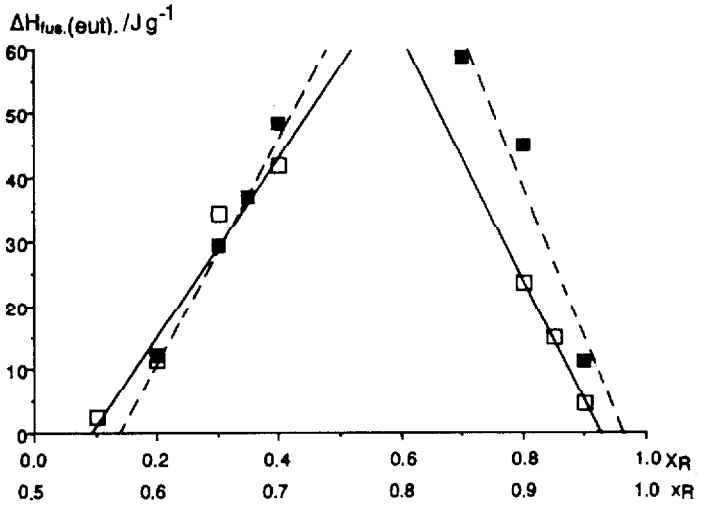

Fig. 5 Tammann diagram of eutectics: □ – physical mixtures, ■ – coprecipitates

dynamic properties of the two enantiomers are identical, Eq. (1) can be used to obtain the position of the eutectics in the *R/S* phase diagram, respectively at x_{R_e}=0.215 and 0.785 for the physical mixtures and 0.195 and 0.805 for the coprecipitates.

The melting temperatures and enthalpies were very similar for the physical mixtures $T_{fus.}$(eut.)=230.3±0.5°C, $\Delta H_{fus.}$(eut.)=112.8±3.7 J g^{-1}, and the coprecipitate $T_{fus.}$(eut.)= 230.8±0.4°C, $\Delta H_{fus.}$(eut.)=117.9±5.2 J g^{-1}.

Discussion

The melting temperatures of eutectics were used to evaluate the stability of the racemic compound by calculating Petterson's coefficient [16].

$$i = [T_{fus.}(RS) - T_{fus.}(\text{eut.})] / [T_{fus.}(R) - T_{fus.}(\text{eut.})] \quad (2)$$

$T_{fus.}(RS)$, $T_{fus.}(R)$ and $T_{fus.}$(eut.) are the melting temperature of the racemic compound, the enantiomers and the eutectics, respectively.

According to Petterson, if i<0.5, this indicates that there is little tendency to form a racemic compound; 0.5<i<1.5 indicates a moderate tendency; i>1.5 a considerable tendency.

As, i=1.19, this confirmed the stability of the racemic compound already established by the calculation of its free enthalpy of formation at $T_{fus.}(R)$, ΔG^{φ}= –3135±752 J mol^{-1} [8], it corresponds to the free enthalpy of the following reaction:

$$R_{\text{cristal}} + S_{\text{cristal}} \rightarrow RS_{\text{cristal}}$$

The eutectic compositions in the *R/S* phase diagram set the range for the racemic compound. The range is broad as it extends from 21.5 to 78.5%*R* for the physical mixture and from 19.5 to 80.5%*R* for the coprecipitates. Under these conditions the ranges for the two enantiomers were too close to hope a resolution by preferential crystallization.

Thus the solid ↔ solid transition cannot contribute to this type of resolution.

The calculation of mixing enthalpy at eutectic composition was used to estimate the deviation from ideality. Generally, for a binary mixture made up of a racemic compound and one of the enantiomers, the mixing enthalpy (ΔH_m) of the liquid phase at the eutectic point is given by the following relationship [17]:

$$\Delta H_m = \Delta H_{fus.}(\text{eut.}) - [X_R \Delta H_{fus.}(R) + X_{RS} \Delta H_{fus.}(RS)] \quad (3)$$

– $\Delta H_{fus.}$(eut.), melting enthalpy of eutectic,
– $\Delta H_{fus.}(R)$ = melting enthalpy of *R* enantiomer,
– $\Delta H_{fus.}(RS)$ = melting enthalpy of *RS* racemic compound,
– X_R et X_{RS} are respectively the mole or mass fractions of the *R* enantiomer and *RS* racemic compound.

The reference state is the melting of the pure compound.

The mixing enthalpies were ΔH_m=–8.9 J g^{-1} for the physical mixtures and –3.7 J g^{-1} for the coprecipitates. The mixing enthalpy of physical mixtures is more exothermic than that of the coprecipitates. The difficulty of homogenization of a physical mixture explains this result.

Only the coprecipitates are in thermodynamic equilibrium. However, physical mixing procedures are homogenization methods used in pharmaceutical industry, especially, to prepare solid dispersions of drugs in excipients or the associations of two drugs [18–19].

The strength of interaction between *R* and *S* was greater than that for the interactions between *R* and *R* or *S* and *S*.

According to Raï *et al.* [17], clusters are formed when $\Delta H_m < 0$ for eutectics constituting of organic compounds. Cluster formation is favoured if the molecule can associate by intermolecular strengths such as hydrogen bonds. As the molecule in our study is a hydrochloride, the amine and the imine functions can generate this kind of interaction.

The low value of ΔH_m showed that the system was not far from ideality particularly for the coprecipitates. To confirm this result we used Prigogine and Defay's Eq. (4) to calculate the melting enthalpy of the racemic compound and compared this with the experimental value.

$$\frac{2\Delta H_{fus.}(RS)}{R}\left[\frac{1}{T} - \frac{1}{T_{fus.}(RS)}\right] = -\ln 4 x_R^1 (1 - x_R^1) \quad (4)$$

x_R^l, $\Delta H_{fus.}(R\,S)$, $T_{fus.}(R\,S)$ have already been defined above. T is the melting temperature of a sample in accordance with its composition x_R^l. R is the gas constant.

If by plotting $\ln x_R^l(1-x_R^l)$ *vs.* $1/T$ a straight line is obtained, the system is ideal and the slope of this straight line is $-2\Delta H_{fus.}(RS)/R$, Fig. 6. For the physical mixture, the equation of this straight line is $y=11.400-6644.5x$ with $r^2=0.996$ and $\Delta H_{fus.}(RS)_{calculated}=110.0$ J g^{-1}; for coprecipitates, $y=12.679-7307.0x$ with $r^2=0.983$ and $\Delta H_{fus.}(RS)_{calculated}=121.0$ J g^{-1}. The values we obtained were therefore similar to the experimental value (124.6±2.4 J g^{-1}). This complementary result confirmed the small deviation from ideality, as already demonstrated by the calculation of the mixing enthalpy.

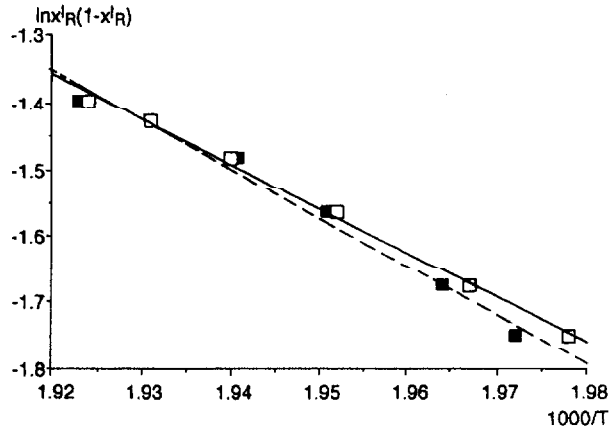

Fig. 6 Test of the Prigogine-Defay equation. Graph of $\ln x_R^l(1-x_R^l)$ *vs.* $1000/T$: □ – physical mixtures, ■ – coprecipitates

From a thermodynamic point of view, the phase diagram may be described as an ideal system. It can be calculated using the Prigogine-Defay equation for the racemic compound liquidus and the Schröeder-Van Laar equation for the enantiomers liquidus.

After rearranging Eq. (4), we obtain the following equation for the racemic compound liquidus which gives the melting temperature of a sample in accordance with its composition x_R^l.

$$T = \frac{1}{\frac{1}{T_{fus.}(RS)} - \frac{R}{2\Delta H_{fus.}(RS)} \ln 4x_R^l(1-x_R^l)} \qquad (5)$$

Using the Shröeder-Van Laar equation, we can describe the enantiomer liquidus by the following relationship:

$$T = \frac{1}{\frac{1}{T_{fus.}(R)} - \frac{R}{\Delta H_{fus.}(R)} \ln x_R^1} \quad (6)$$

T, $\Delta H_{fus.}(R)$, x_R^1, R were defined above. The eutectic position (x_R^1) and its melting temperature (T) may be calculated from liquidus Eqs (5) and (6). This gives a system of two equations with two unknowns (x_R^1, T).

Table 5 Temperature and composition of two eutectics x_{R_1} and x_{R_2}

Eutectic	x_{R_1}	x_{R_2}	T/°C
Physical mixture	0.795	0.205	230.3±0.5
Coprecipitate	0.805	0.195	230.8±0.4
Calculated	0.815	0.185	230.5

The results are reported in Table 5 and the phase diagram is shown in Fig. 2a, b. The calculated values are given next to the experimental values.

Conclusions

Study of the $R(+)$-$S(-)$ phase diagram of efaroxan hydrochloride confirmed the results obtained previously.

The racemate formed by an equimolar mixture of the two enantiomers was a racemic compound thermodynamically stable over a broad range. It could not be resolved by preferential crystallization. The low values obtained for the mixing enthalpies at the melting temperature of the eutectics reflected a small deviation from ideality.

This result was confirmed by the melting enthalpies of the racemic compound calculated from the Prigogine-Defay equation. The calculated value was close to the experimental value. The small deviation from ideality confirmed by this last result led us to calculate the phase diagram assuming that the system is ideal. The agreement of the calculated phase diagram and the experimental diagrams justifies our hypothesis.

References

1 M. F. Balandrin, J. A. Klocke, E. S. Wurtele and W. H. Bolliger, Science, 228 (1985) 1154.
2 M. Simonyi, Med. Res. Rev., 4 (1984) 359.
3 D. E. Drayer. In: M. M. Reidenberg, S; Erill, eds. Drug Protein Binding. New York: Praeger Publishers, 1986, p. 332.
4 E. J. Ariens, Eur. J. Pharmacol., 26 (1984) 663.
5 K. Williams and E. Lee, Drugs, 30 (1985) 333.

6 C. Belin, A. Chauvet, J. M. Leloup, J. P. Ribet and J. L. Maurel, Acta Cryst., C51(1995) 2439.
7 S. Tellez, F. Colpaert and M. Marien, Eur. J. Pharmacol., 277 (1995) 113.
8 R. Pena, A. Chauvet, J. Masse, J. P. Ribet and J. L. Maurel, J. Thermal Anal. Cal., 53 (1998) 123.
9 J. Jacques, J. Collet and S. H. Wilen: Enantiomers, Racemates and Resolutions, Wiley & Sons, New York, 1981.
10 A. Collet, M. J. Brienne and J. Jacques, Chem. Rev., 80 (1980) 215.
11 I. Prigogine and R. Defay, Chemical Thermodynamics, Longman, London, 1954.
12 F. Gronvold, J. Chem. Thermodyn., 25(9) (1993) 1133.
13 M. Kuhnert-Brandstätter, Thermomicroscopy in the Analysis of Pharmaceuticals, Ed. Pergamon Press, 1971.
14 R. L. Scott, J. Chem. Soc. Far. Trans., 2,3 (1977) 356.
15 C. Belin, R. Pena, A. Chauvet, J. P. Ribet and J. L. Maurel, Acta Cryst., C54, 3 (1998) IUC 9800004.
16 M. Leclerc, A. Collet and J. Jacques, Tetrahedron Letters, 32 (1976) 828.
17 U. S. Raï, K. D. Mandal and N. P. Singh, J. Thermal Anal., 35 (1989) 1687.
18 K. Sekiguchi, I. Himuro, I. Horikoshi, T. Tsukada, T. Okamoto and Y. Yotsuyanagi, Chem. Pharm. Bull., 17 (1) (1969) 191.
19 F. Lacoulonche, A. Chauvet, J. Masse, Int. J. Pharm., 153 (1997) 167.